

# Phase and Thermal Driven Transport across T-Shaped Double Quantum Dot Josephson Junction

Bhupendra Kumar <sup>\*</sup>, Sachin Verma <sup>†</sup> and Ajay <sup>‡</sup>

Department of Physics, Indian Institute of Technology, Roorkee, Uttarakhand, India

August 8, 2022

The phase and thermal driven transport properties of the T-shaped double quantum dot Josephson junction are analyzed by using the Keldysh non-equilibrium Green's function technique. We began with investigating the impact of interdot hopping on Andreev bound states and Josephson supercurrent. When a small thermal bias is applied across the superconducting leads, the system exhibit a finite thermal response which is primarily due to the, thermally induced, quasi-particle current. The behavior of Josephson supercurrent and quasi-particle current flowing through the quantum dots is examined for various interdot hopping and thermal biasing. Finally, the system is considered in an open circuit configuration where the thermally driven quasi-particle current is compensated by the phase driven Josephson supercurrent and thermophase effect is observed. The effect of interdot hopping, onsite Coulomb interaction, and the position of quantum dot energy level on the thermophase Seebeck coefficient is investigated.

**Keywords:** Quantum dots, T-shaped Josephson junction, Coulomb correlation, thermophase Seebeck effect

## 1 Introduction

A quantum dot (QD)-based Josephson junction is made up of two Bardeen-Cooper-Schrieffer (BCS) superconducting leads separated by a quantum dot. A DC Josephson supercurrent can flow across the junction without applying potential difference, as the Josephson supercurrent largely depends on the phase difference between the superconductors [1, 2]. Quantum dots have discrete energy levels and can be controlled by tuning their gate voltage or by changing the size of quantum dot [3, 4]. Single-electron (quasi-particle) tunneling and cooper pair tunneling are responsible for charge transport in quantum dot-based Josephson junctions. Charge transport in these single quantum dot-based Josephson junctions have been studied extensively both theoretically [5, 6, 7, 8, 9, 10, 11, 12, 13] as well as experimentally [14, 15, 16, 17, 18, 19, 20, 21]. Using quantum dots allow one to control the current flowing through Josephson junctions. Further, various authors have explored the charge transport properties of double quantum dot Josephson junctions. In such junctions the double quantum dot are coupled with superconducting leads in series, parallel and T-shaped geometry [22, 23, 24, 25, 26, 27, 28, 29]. References [30, 31, 32] provides a recent detailed reviews on the charge transport properties of single and double quantum dot based Josephson junctions.

On the other hand, due to the limited temperature range the thermal transport properties of the ordinary S-I-S Josephson junction and quantum dot-based junctions have not been widely explored. Despite this limitation, the thermal transport properties of Josephson junctions are recently attracting great attention [33, 34, 35, 36, 37, 38, 39]. Recently, very few studies has been conducted on the thermal transport properties of quantum dot-based Josephson junctions i.e when both the leads are superconducting [40, 41]. Further, the thermoelectric transport properties of systems where the quantum dot is coupled between normal metal and BCS superconductor (N-QD-S) [42, 43, 44] and ferromagnet and BCS superconductor (F-QD-S) [45, 46, 47, 48] have been studied recently. Further the thermoelectric transport properties of multi-dot and multi-terminal systems with one superconducting lead are also gaining attention [49, 50, 51, 52, 53].

---

<sup>\*</sup>bhupendra.k@ph.iitr.ac.in

<sup>†</sup>sverma2@ph.iitr.ac.in

<sup>‡</sup>ajay@ph.iitr.ac.in

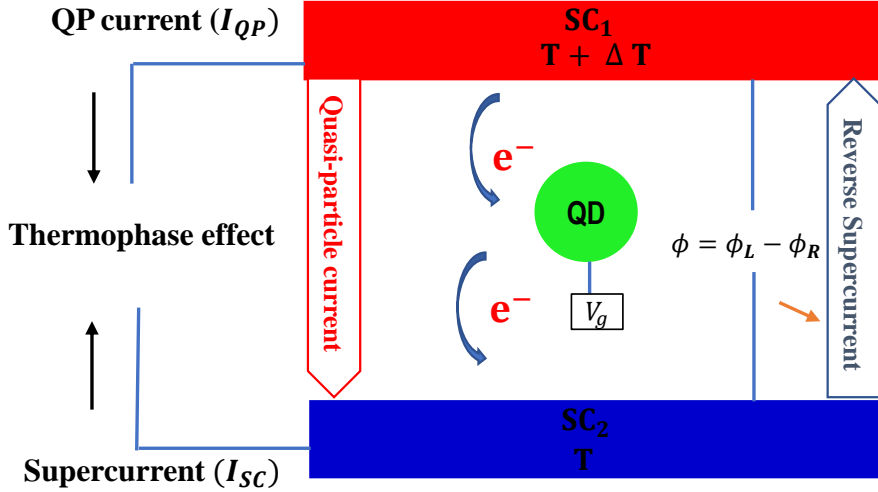


Figure 1: Schematic diagram showing the origin of thermophase Seebeck effect. The cancellation of quasi-particle current, induced by temperature difference, by phase driven reverse supercurrent is the origin of thermophase.

Phase and thermal driven transport properties of quantum dot-based Josephson junctions can be analyzed through a combination of three currents: quasi-particle current, interference current, and pair current [54]. A thermal gradient induces the quasi-particle current to flow across the junction. Quasi-particle is the only current that contributes to thermal transport in the S-QD-S system. The interference current, which is due to coupling between quasi-particle and condensate shows no contribution to thermal transport and will be ignored in the present study. The pair current or Josephson supercurrent flows across the junction in absence of voltage difference or temperature difference between the superconducting leads. This Josephson current depends on the phase difference between the superconducting leads. In reference [40, 41] author demonstrates that quantum dot-based Josephson junction shows a significant thermal response on applying the thermal biasing across the superconducting leads. By applying the thermal biasing across the superconducting leads, there appears to be a phase gradient across the superconductors. Therefore, a supercurrent will flow across the junction and it will counterbalance the thermally induced quasi-particle current. This is the open circuit configuration for S-QD-S system i.e. total current  $I_C = 0$ . The cancellation of quasi-particle current by reverse supercurrent, is the origin of concept of thermophase Seebeck effect in quantum dot based Josephson junctions as shown by the schematic diagram in figure 1.

In the present work, we provide a study of the low-temperature phase and thermal driven transport properties of system where double quantum dot are coupled with two superconducting leads in T-shaped geometry (figure 2). In this configuration the main quantum dot ( $QD_1$ ) is directly coupled with the leads and the side quantum dot ( $QD_2$ ) is coupled with the main dot but not with the superconducting leads. To study the thermal transport properties of T-shaped double quantum dot Josephson junction, we have employed Keldysh non-equilibrium Green's function technique within the Hartree – Fock mean field approximation [55, 56]. First, We have studied the interdot hopping dependence of Andreev Bound States (ABS) and supercurrent. Next, total current (which is the combination of quasi-particle current and Josephson supercurrent) is calculated for different temperature differences  $\Delta T$  and interdot hopping ( $t$ ). Finally, thermophase Seebeck coefficient (TPSC) for T-shaped double quantum dot Josephson junction is analyzed. Since, both the leads are superconductors, so we have taken into account the temperature dependence of the superconducting gap ( $\Delta_\alpha$ ) having a background temperature always less than the superconducting critical temperature  $T_c$ .

This paper can be read in the following order: in the preceding section 2, we provide a detailed description of model Hamiltonian and theoretical formalism. Section 3, discusses numerical results. Lastly, section 4 concludes the present work.

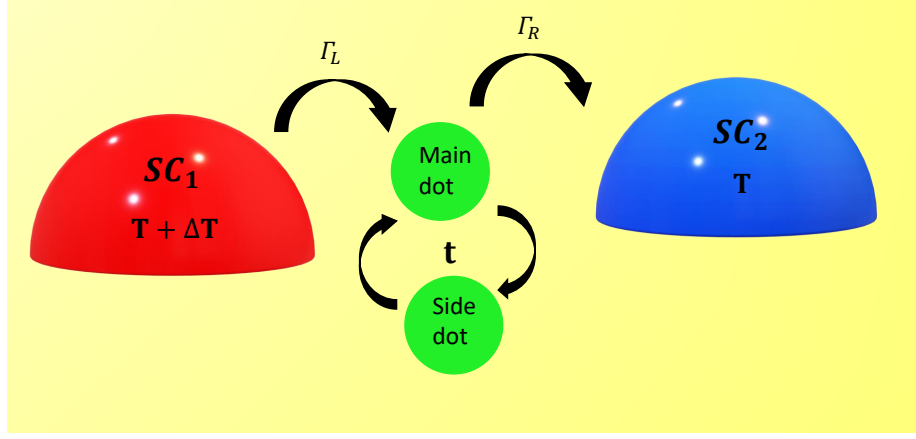


Figure 2: Schematic diagram for double quantum dot in T-shaped geometry coupled with superconducting leads. Main dot ( $QD_1$ ) is directly coupled with superconducting leads while the side dot ( $QD_2$ ) is only coupled with main dot.

## 2 Model Hamiltonian and theoretical formalism

To calculate the transport properties of T-shaped double quantum dot Josephson junction, we use the generalized Anderson + BCS Hamiltonian in second quantization formalism.

$$\hat{H} = \hat{H}_{leads} + \hat{H}_{QD} + \hat{H}_{tunnel} + \hat{H}_{interdot-hopping} \quad (1)$$

where

$$\begin{aligned} \hat{H}_{leads} &= \sum_{k\sigma,\alpha} \epsilon_{k\alpha} c_{k\sigma,\alpha}^\dagger c_{k\sigma,\alpha} - \left( \sum_{k\alpha} \Delta_\alpha c_{k\uparrow,\alpha}^\dagger c_{-k\downarrow,\alpha}^\dagger + h.c \right) \\ \hat{H}_{QD} &= \sum_{i=1}^{i=2} \sum_{\sigma} \epsilon_{d_{i\sigma}} d_{i\sigma}^\dagger d_{i\sigma} + \sum_{i=1}^{i=2} U_i n_{i\sigma} n_{i-\sigma} \\ \hat{H}_{tunnel} &= \sum_{k\sigma,\alpha} V_{k,\alpha} c_{k\sigma,\alpha}^\dagger d_{1\sigma} + h.c \\ \hat{H}_{interdot-hopping} &= \sum_{\sigma} t (d_{1\sigma}^\dagger d_{2\sigma} + h.c) \end{aligned}$$

where h.c stands for Hermitian conjugate.

$\hat{H}_{leads}$  is the Hamiltonian for left and right superconducting leads ( $\alpha \in L, R$ ). The first term, describes the free electrons in the superconducting leads;  $c_{k\sigma,\alpha}^\dagger$  ( $c_{k\sigma,\alpha}$ ) is creation (annihilation) operator of electron with spin  $\sigma$  and wave vector  $\vec{k}$  and energy  $\epsilon_{k,\alpha}$ . The second term in  $\hat{H}_{leads}$  is BCS term and gives the information about interaction between cooper pair with superconducting gap energy  $\Delta_\alpha$ .

$\hat{H}_{QD}$  is the Hamiltonian for main dot ( $QD_1$ ) and side dot ( $QD_2$ ).  $QD_1$  ( $i=1$ ) and  $QD_2$  ( $i=2$ ) has energy  $\epsilon_{d_{i\sigma}}$  with  $d_{i\sigma}^\dagger$  ( $d_{i\sigma}$ ) as the fermionic creation operator (annihilation operator) of electrons with spin  $\sigma$  and  $n_{d_{i\sigma}} = d_{i\sigma}^\dagger d_{i\sigma}$  is the number operator. Also, the finite onsite electron-electron Coulomb interaction (correlation) with a strength of  $U_i$  is considered. We have neglected interdot onsite coulomb interaction  $U_{12}$  for simplification.

$\hat{H}_{tunnel}$  is tunneling Hamiltonian between the energy level of main dot and superconducting leads with interaction strength  $V_{k_1,\alpha}$ . Further, we have consider the symmetric coupling strength of  $QD_1$  to the left and right leads i.e.  $V_{k_1;L} = V_{k_1;R}$ .

The last term  $\hat{H}_{interdot-hopping}$  describes the interaction of electrons of two quantum dots via a hopping like term of strength  $t$ . Note that, there is no direct interaction between superconducting leads and  $QD_2$ .

Bogoliubov transformation is used to diagonalize the BCS part of the Hamiltonian. For this we introduce a new fermionic quasiparticle operator  $\beta$  with coefficient  $u_k$  and  $v_k$  which satisfies the normalization condition  $|u_k|^2 + |v_k|^2 = 1$

$$c_{k\uparrow} = u_k^* \beta_{k\uparrow} + v_k \beta_{-k\downarrow}^\dagger \quad (2)$$

$$c_{-k\downarrow}^\dagger = u_k \beta_{-k\downarrow}^\dagger - v_k^* \beta_{k\uparrow} \quad (3)$$

By replacing the fermionic operator  $c_{k\uparrow}$  and  $c_{-k\downarrow}^\dagger$  with new quasi-particle operator, we get the effective Hamiltonian

$$\begin{aligned} \hat{H} = & \sum_{k\alpha} E_{k\alpha} (\beta_{k\uparrow,\alpha}^\dagger \beta_{k\uparrow,\alpha} + \beta_{-k\downarrow,\alpha}^\dagger \beta_{-k\downarrow,\alpha}) \\ & + \sum_{k\alpha} (V_{k\alpha} u_k^* \beta_{k\uparrow,\alpha}^\dagger d_{1\uparrow} + V_{k\alpha} u_k^* \beta_{-k\downarrow,\alpha}^\dagger d_{1\downarrow}) \\ & + \sum_{k\alpha} (V_{k\alpha}^* u_k d_{1\uparrow}^\dagger \beta_{k\uparrow,\alpha} + V_{k\alpha}^* u_k d_{1\downarrow}^\dagger \beta_{-k\downarrow,\alpha}) \\ & + \sum_{k\alpha} V_{k\alpha} v_k (\beta_{-k\downarrow,\alpha} d_{1\uparrow} - \beta_{k\uparrow,\alpha} d_{1\downarrow}) \\ & + \sum_{k\alpha} V_{k\alpha}^* v_k^* (d_{1\uparrow}^\dagger \beta_{-k\downarrow,\alpha}^\dagger - d_{1\downarrow}^\dagger \beta_{k\uparrow,\alpha}^\dagger) \\ & + \epsilon_{d_1} (d_{1\uparrow}^\dagger d_{1\uparrow} + d_{1\downarrow}^\dagger d_{1\downarrow}) \\ & + \epsilon_{d_2} (d_{2\uparrow}^\dagger d_{2\uparrow} + d_{2\downarrow}^\dagger d_{2\downarrow}) \\ & + t (d_{1\uparrow}^\dagger d_{2\uparrow} + d_{1\downarrow}^\dagger d_{2\downarrow} + d_{2\uparrow}^\dagger d_{1\uparrow} + d_{2\downarrow}^\dagger d_{1\downarrow}) \\ & + \sum_{i=1}^{i=2} U_i d_{i\uparrow}^\dagger d_{i\uparrow} d_{i\downarrow}^\dagger d_{i\downarrow} \end{aligned} \quad (4)$$

where  $E_{k\alpha} = \sqrt{\epsilon_{k\alpha}^2 + |\Delta_\alpha|^2}$  is excitation quasi-particle energy of the superconducting leads. The coefficients  $u_k$  and  $v_k$  can be expressed as

$$|u_k|^2 = \frac{1}{2} \left( 1 + \frac{\epsilon_{k,\alpha}}{\sqrt{\epsilon_{k,\alpha}^2 + |\Delta_\alpha|^2}} \right) \quad (5)$$

$$|v_k|^2 = \frac{1}{2} \left( 1 - \frac{\epsilon_{k,\alpha}}{\sqrt{\epsilon_{k,\alpha}^2 + |\Delta_\alpha|^2}} \right) \quad (6)$$

To deal with onsite Coulomb correlation, we use the Hartree-Fock (HF) mean field approximation [57]. Within HF mean field approximation, the quartic term can be simplified as:

$$\begin{aligned} \sum_{i=1}^{i=2} U_i n_{d_{i\uparrow}} n_{d_{i\downarrow}} = & U_1 \langle n_{d_{1\uparrow}} \rangle n_{d_{1\downarrow}} + U_1 \langle n_{d_{1\downarrow}} \rangle n_{d_{1\uparrow}} \\ & + U_1 \langle d_{1\downarrow}^\dagger d_{1\uparrow}^\dagger \rangle d_{1\uparrow} d_{1\downarrow} + U_1 \langle d_{1\uparrow} d_{1\downarrow} \rangle d_{1\downarrow}^\dagger d_{1\uparrow}^\dagger \\ & + U_2 \langle n_{d_{2\uparrow}} \rangle n_{d_{2\downarrow}} + U_2 \langle n_{d_{2\downarrow}} \rangle n_{d_{2\uparrow}} \\ & + U_2 \langle d_{2\downarrow}^\dagger d_{2\uparrow}^\dagger \rangle d_{2\uparrow} d_{2\downarrow} + U_2 \langle d_{2\uparrow} d_{2\downarrow} \rangle d_{2\downarrow}^\dagger d_{2\uparrow}^\dagger \end{aligned} \quad (7)$$

where  $\langle n_{d_{i\sigma}} \rangle$  is the average of occupation in the  $i^{th}$  dot and the  $\langle d_{i\downarrow}^\dagger d_{i\uparrow}^\dagger \rangle$  or  $\langle d_{i\uparrow} d_{i\downarrow} \rangle$  represents the qualitative measure of the superconducting induced on-dot pairing. At finite temperature the average superconducting pairing correlation terms i.e.  $\langle d_{i\bar{\sigma}}^\dagger d_{i\sigma}^\dagger \rangle$  and  $\langle d_{i\sigma} d_{i\bar{\sigma}} \rangle$  are negligible and only average occupation  $\langle n_{d_{i\sigma}} \rangle$  need to be calculated self-consistently [40, 43, 44]. Thus within the HF mean field approximation the Hamiltonian in

equation (4) is simplified as

$$\begin{aligned}
\hat{H} = & \sum_{k\alpha} E_{k\alpha} (\beta_{k\uparrow,\alpha}^\dagger \beta_{k\uparrow,\alpha} + \beta_{-k\downarrow,\alpha}^\dagger \beta_{-k\downarrow,\alpha}) \\
& + \sum_{k\alpha} (V_{k\alpha} u_k^* \beta_{k\uparrow,\alpha}^\dagger d_{1\uparrow} + V_{k\alpha} u_k^* \beta_{-k\downarrow,\alpha}^\dagger d_{1\downarrow}) \\
& + \sum_{k\alpha} (V_{k\alpha}^* u_k d_{1\uparrow}^\dagger \beta_{k\uparrow,\alpha} + V_{k\alpha}^* u_k d_{1\downarrow}^\dagger \beta_{-k\downarrow,\alpha}) \\
& + \sum_{k\alpha} V_{k\alpha} v_k (\beta_{-k\downarrow,\alpha} d_{1\uparrow} - \beta_{k\uparrow,\alpha} d_{1\downarrow}) \\
& + \sum_{k\alpha} V_{k\alpha}^* v_k (d_{1\uparrow}^\dagger \beta_{-k\downarrow,\alpha}^\dagger - d_{1\downarrow}^\dagger \beta_{k\uparrow,\alpha}^\dagger) \\
& + \epsilon_{d_1} (d_{1\uparrow}^\dagger d_{1\uparrow} + d_{1\downarrow}^\dagger d_{1\downarrow}) \\
& + \epsilon_{d_2} (d_{2\uparrow}^\dagger d_{2\uparrow} + d_{2\downarrow}^\dagger d_{2\downarrow}) \\
& + t (d_{1\uparrow}^\dagger d_{2\uparrow} + d_{1\downarrow}^\dagger d_{2\downarrow} + d_{2\uparrow}^\dagger d_{1\uparrow} + d_{2\downarrow}^\dagger d_{1\downarrow}) \\
& + U_1 \langle n_{d_{1\uparrow}} \rangle n_{d_{1\downarrow}} + U_1 \langle n_{d_{1\downarrow}} \rangle n_{d_{1\uparrow}} \\
& + U_2 \langle n_{d_{2\uparrow}} \rangle n_{d_{2\downarrow}} + U_2 \langle n_{d_{2\downarrow}} \rangle n_{d_{2\uparrow}}
\end{aligned} \tag{8}$$

where  $\langle n_{d_{1\sigma}} \rangle$ ,  $\langle n_{d_{2\sigma}} \rangle$  can be calculated self-consistently with the the help of following equation [55].

$$\langle n_{d_{i\sigma}} \rangle = -\frac{1}{\pi} \int_{-\infty}^0 \text{Im} \{ \langle \langle d_{i\sigma} | d_{i\sigma}^\dagger \rangle \rangle \} d\omega \tag{9}$$

We have used Green's equation of motion method (EOM) to solve the above effective Hamiltonian. To calculate the spectral and transport properties of T-shaped double quantum dot Josephson junction system, we need single-particle retarded Green's function which is defined as [55, 56, 58]

$$G_{d\sigma}^r(t) = \langle \langle d_\sigma(t); d_\sigma^\dagger(0) \rangle \rangle = -i\theta(t) \langle [d_\sigma(t), d_\sigma^\dagger(0)]_+ \rangle$$

Fourier transform of retarded Green's function should satisfy the equation of motion

$$\omega \langle \langle d_\sigma | d_\sigma^\dagger \rangle \rangle_\omega = \langle \{ d_\sigma, d_\sigma^\dagger \}_+ \rangle + \langle \langle [d_\sigma, H]_- | d_\sigma^\dagger \rangle \rangle_\omega \tag{10}$$

In Nimbu space, the retarded Green's function of quantum dots can be represented as,

$$\begin{pmatrix} \langle \langle d_{i\uparrow} | d_{i\uparrow}^\dagger \rangle \rangle_\omega & \langle \langle d_{i\uparrow} | d_{i\downarrow} \rangle \rangle_\omega \\ \langle \langle d_{i\downarrow}^\dagger | d_{i\uparrow}^\dagger \rangle \rangle_\omega & \langle \langle d_{i\downarrow}^\dagger | d_{i\downarrow} \rangle \rangle_\omega \end{pmatrix} \tag{11}$$

To calculate the transport properties of the T-shaped double quantum dot based Josephson junction, we required the Green's function for the main dot i.e.  $G_{11}^\sigma(\omega) = \langle \langle d_{1\sigma} | d_{1\sigma}^\dagger \rangle \rangle$  and second dot i.e.  $G_{22}^\sigma(\omega) = \langle \langle d_{2\sigma} | d_{2\sigma}^\dagger \rangle \rangle$ . The other terms of Green' function matrix can be calculate with the help of following relations.

$$\langle \langle d_{i\downarrow}^\dagger | d_{i\downarrow} \rangle \rangle_\omega = - \left\{ \langle \langle d_{i\uparrow} | d_{i\uparrow}^\dagger \rangle \rangle_{(-\omega)} \right\}^* \tag{12}$$

$$\langle \langle d_{i\uparrow} | d_{i\downarrow} \rangle \rangle_\omega = \left\{ \langle \langle d_{i\downarrow}^\dagger | d_{i\uparrow}^\dagger \rangle \rangle_{(-\omega)} \right\}^* \tag{13}$$

We obtained the following coupled equations of the main dot  $QD_1$  using the Green's function EOM technique.

$$\begin{aligned}
(\omega - E_{d_{1\uparrow}}) \langle \langle d_{1\uparrow} | d_{1\uparrow}^\dagger \rangle \rangle = & 1 + \sum_{k\alpha} V_{k\alpha} u_k^* \langle \langle \beta_{k\uparrow,\alpha} | d_{1\uparrow}^\dagger \rangle \rangle \\
& + \sum_{k\alpha} V_{k\alpha} v_k \langle \langle \beta_{-k\downarrow,\alpha}^\dagger | d_{1\uparrow}^\dagger \rangle \rangle \\
& + t \langle \langle d_{2\uparrow} | d_{1\uparrow}^\dagger \rangle \rangle
\end{aligned} \tag{14}$$

$$\begin{aligned}
(\omega - E_{k\alpha})\langle\langle\beta_{k\uparrow,\alpha}|d_{1\uparrow}^\dagger\rangle\rangle &= \sum_{k\alpha} V_{k\alpha}^* u_k \langle\langle d_{1\uparrow}|d_{1\uparrow}^\dagger\rangle\rangle \\
&+ \sum_{k\alpha} V_{k\alpha} v_k \langle\langle d_{1\downarrow}|d_{1\uparrow}^\dagger\rangle\rangle
\end{aligned} \tag{15}$$

$$\begin{aligned}
(\omega + E_{k\alpha})\langle\langle\beta_{-k\downarrow,\alpha}^\dagger|d_{1\uparrow}^\dagger\rangle\rangle &= \sum_{k\alpha} V_{k\alpha}^* v_k^* \langle\langle d_{1\uparrow}|d_{1\uparrow}^\dagger\rangle\rangle \\
&- \sum_{k\alpha} V_{k\alpha} u_k^* \langle\langle d_{1\downarrow}|d_{1\uparrow}^\dagger\rangle\rangle
\end{aligned} \tag{16}$$

$$\begin{aligned}
(\omega + E_{d_{1\downarrow}})\langle\langle d_{1\downarrow}^\dagger|d_{1\uparrow}^\dagger\rangle\rangle &= \sum_{k\alpha} V_{k\alpha}^* v_k^* \langle\langle\beta_{k\uparrow,\alpha}|d_{1\uparrow}^\dagger\rangle\rangle \\
&+ \sum_{k\alpha} V_{k\alpha}^* u_k \langle\langle\beta_{-k\downarrow,\alpha}^\dagger|d_{1\uparrow}^\dagger\rangle\rangle \\
&- t \langle\langle d_{2\downarrow}^\dagger|d_{1\uparrow}^\dagger\rangle\rangle
\end{aligned} \tag{17}$$

$$(\omega - E_{d_{2\uparrow}})\langle\langle d_{2\uparrow}|d_{1\uparrow}^\dagger\rangle\rangle = t \langle\langle d_{1\uparrow}|d_{1\uparrow}^\dagger\rangle\rangle \tag{18}$$

$$(\omega - E_{d_{2\downarrow}})\langle\langle d_{2\downarrow}|d_{1\uparrow}^\dagger\rangle\rangle = -t \langle\langle d_{1\downarrow}|d_{1\uparrow}^\dagger\rangle\rangle \tag{19}$$

where  $E_{d_{i\sigma}} = \epsilon_{d_i} + U_i \langle n_{d_{i\bar{\sigma}}} \rangle$ . After solving these coupled equations the expression for single particle retarded Green's function ( $\langle\langle d_{1\uparrow}|d_{1\uparrow}^\dagger\rangle\rangle$ ) ( $G_{d_{11}}^r(\omega)$ ) for main dot can be written as:

$$G_{d_{11},\uparrow}^r(\omega) = \frac{\omega + E_{d_{1\downarrow}} - \frac{t^2}{\omega + E_{d_{2\downarrow}}} - I_1}{(\omega + E_{d_{1\downarrow}} - \frac{t^2}{\omega + E_{d_{2\downarrow}}} - I_1)(\omega - E_{d_{1\uparrow}} - \frac{t^2}{\omega - E_{d_{2\uparrow}}} - I_2) - (I_3)^2} \tag{20}$$

In above Green's function (Eq. 20)  $I_1$ ,  $I_2$  are the diagonal, and  $I_3$  is the off-diagonal part of self-energy, which corresponds to the induced pairing, due to the coupling between the quantum dot and superconducting leads. The expressions for  $I_1$ ,  $I_2$  and  $I_3$  are

$$I_1 = |V_{k\alpha}|^2 \sum_{k\alpha} \left( \frac{|u_k|^2}{\omega + E_{k\alpha}} + \frac{|v_k|^2}{\omega - E_{k\alpha}} \right) \tag{21}$$

$$I_2 = |V_{k\alpha}|^2 \sum_{k\alpha} \left( \frac{|u_k|^2}{\omega - E_{k\alpha}} + \frac{|v_k|^2}{\omega + E_{k\alpha}} \right) \tag{22}$$

$$I_3 = |V_{k\alpha}|^2 \sum_{k\alpha} u_k v_k^* \left( \frac{1}{\omega - E_{k\alpha}} - \frac{1}{\omega + E_{k\alpha}} \right) \tag{23}$$

Transforming the summation into integration and by defining the tunneling rate  $\Gamma_\alpha = 2\pi\rho_0|V_{k\alpha}|^2$  where  $\rho_0$  is density of states in normal metallic state, we obtained the following values for  $I_1$ ,  $I_2$  and  $I_3$ :

$$I_1 = I_2 = - \sum_{\alpha \in L,R} \frac{\Gamma_\alpha \omega}{\sqrt{|\Delta_\alpha|^2 - \omega^2}} \tag{24}$$

$$I_3 = - \sum_{\alpha \in L,R} \frac{\Gamma_\alpha \Delta_\alpha}{\sqrt{|\Delta_\alpha|^2 - \omega^2}} \tag{25}$$

Finally the single particle retarded Green's function for main dot ( $QD_1$ ) can be written as :

$$G_{d_{11},\uparrow}^r(\omega) = \frac{\omega + E_{d_{1\downarrow}} - \frac{t^2}{\omega + E_{d_{2\downarrow}}} + \sum_\alpha \frac{\Gamma_\alpha \omega}{\sqrt{|\Delta_\alpha|^2 - \omega^2}}}{\left[ (\omega + E_{d_{1\downarrow}} - \frac{t^2}{\omega + E_{d_{2\downarrow}}} + \sum_\alpha \frac{\Gamma_\alpha \omega}{\sqrt{|\Delta_\alpha|^2 - \omega^2}})(\omega - E_{d_{1\uparrow}} - \frac{t^2}{\omega - E_{d_{2\uparrow}}} + \sum_\alpha \frac{\Gamma_\alpha \omega}{\sqrt{|\Delta_\alpha|^2 - \omega^2}}) - (\sum_\alpha \frac{\Gamma_\alpha \Delta_\alpha}{\sqrt{|\Delta_\alpha|^2 - \omega^2}})^2 \right]} \tag{26}$$

In the same way, we have solved the coupled equations for the side dot and obtained the single particle retarded Green's function  $G_{d_{22}}^r$  for side dot ( $QD_2$ ).

$$G_{d_{22},\uparrow}^r(\omega) = \langle\langle d_{2\uparrow}|d_{2\uparrow}^\dagger \rangle\rangle = \frac{\omega + E_{d_{2\downarrow}} - \frac{t^2 K}{KL-M^2}}{(\omega + E_{d_{2\downarrow}} - \frac{t^2 K}{KL-M^2})(\omega - E_{d_{2\uparrow}} - \frac{t^2 L}{KL-M^2}) - \left(\frac{t^2 M}{KL-M^2}\right)^2} \quad (27)$$

where

$$K = \omega - E_{d_{1\uparrow}} + \sum_{\alpha} \frac{\Gamma_{\alpha}\omega}{\sqrt{|\Delta_{\alpha}|^2 - \omega^2}} \quad (28)$$

$$L = \omega + E_{d_{1\downarrow}} + \sum_{\alpha} \frac{\Gamma_{\alpha}\omega}{\sqrt{|\Delta_{\alpha}|^2 - \omega^2}} \quad (29)$$

$$M = - \sum_{\alpha} \frac{\Gamma_{\alpha}\Delta_{\alpha}}{\sqrt{|\Delta_{\alpha}|^2 - \omega^2}} \quad (30)$$

The other elements in the matrix can be calculated with the help of relations given in Eq. (12) and (13).

As discussed in section 1, for quantum dot based Josephson junction, we can distribute the current in three parts: quasi-particle current  $I_{QP}$ , Josephson current  $I_{SC}$ , and interference term pair-QP  $I_{pair-QP}$ .

$$I = I_{QP}(\epsilon_{di}, \phi, T, \Delta T) + I_{pair-QP}(\epsilon_{di}, \phi, T, \Delta T) \cos^2 \frac{\phi}{2} + I_{SC}(\epsilon_{di}, \phi, T, \Delta T) \sin(\phi) \quad (31)$$

The first term is quasi-particle current and is responsible for thermal transport in this system. The second term has no contribution to thermal transport. The third term in current is due to cooper pair tunneling and responsible for the supercurrent in system. The quasi-particle and supercurrent can be simplified as follow [40, 59]:

$$I_{QP} = \frac{e}{h} \sum_{\sigma} \int_{-\infty}^{\infty} d\omega \frac{df(\omega)}{dT} \Gamma_{\alpha}[\rho(\omega)] \text{Im}[-G_{d\sigma}^r(\omega)] \Delta T \quad (32)$$

$$I_{SC} = \frac{e}{h} \sum_{\sigma} \int_{-\infty}^{\infty} d\omega f(\omega) \frac{\Delta_{\alpha}^2 \Gamma_{\alpha}^2}{\omega^2 - \Delta_{\alpha}^2} \text{Im}\left[-\frac{1}{A(\omega)}\right] \quad (33)$$

where  $\Gamma$  is the symmetric tunneling rate between main dot and superconducting leads (i.e.  $\Gamma_L = \Gamma_R = \Gamma$ ),  $f(\omega)$  is the Fermi distribution function,  $\Delta T$  is the thermal biasing between both superconducting leads,  $\rho(\omega)$  is the density of states,  $A(\omega)$  is the denominator of retarded Green's function and  $\Delta_{\alpha}$  is the temperature dependent superconducting energy gap which is given by [41]

$$\Delta_{\alpha}(T_{\alpha}) = \Delta_0 \tanh \left\{ 1.74 \sqrt{\left(\frac{k_B T_c}{k_B T_{\alpha}} - 1\right)} \right\}$$

$\Delta_0$  is the superconducting gap at absolute zero temperature,  $T_c$  is superconducting critical temperature,  $T_{\alpha}$  is the temperature of superconducting leads and  $k_B$  is the Boltzman constant. In section 1, we have already discussed the origin of thermophase effect. Within the linear response regime (thermal gradient between superconducting leads will be small,  $\Delta T \rightarrow 0$ ), the thermophase Seebeck coefficient  $S_{\phi}$  is defined analogous to the thermovoltage Seebeck coefficient and can be simplified using eq. (31)

$$S_{\phi} = - \left( \frac{\Delta\phi}{\Delta T} \right)_{I=0} = \frac{dI_{QP}/d\Delta T}{I_{SC}} \quad (34)$$

### 3 Results and discussion

In this section, we present the numerical results and discussion for T-shaped double quantum dot Josephson junction. Transport properties are discussed for a uncorrelated and correlated quantum dots. The superconducting gap at absolute zero temperature ( $\Delta_0$ ) is considered as the energy unit, where  $\Delta_0$  is in meV.

In figure 3, we plot the energy of Andreev Bound states (ABS) and Josephson current as a function of superconducting phase difference ( $\phi$ ) for different values of interdot hopping ( $t$ ). First, when  $QD_2$  is decoupled

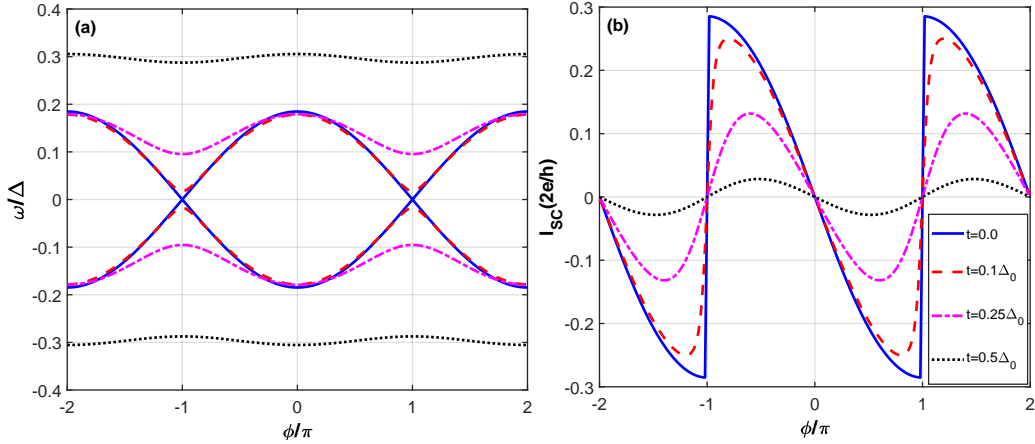


Figure 3: (a) Energy of Andreev bound states and (b) Josephson current as a function of superconducting phase difference ( $\phi$ ) for different value of interdot hopping ( $t$ ) at absolute zero temperature. The other parameters are  $\Gamma = 0.1\Delta_0$ ,  $\epsilon_{d_1} = 0$ ,  $\epsilon_{d_2} = 0.5\Delta_0$ .

from  $QD_1$  i.e.  $t=0$ , the system shows the properties of usual S-QD-S Josephson junction. In this case, the supercurrent is discontinuous at  $\phi = \pm\pi$  and upper and lower ABS crosses the Fermi energy ( $\omega = 0$ ). Thus for  $t=0$ , the system acts as perfect transmitting channel. When  $QD_2$  is coupled with  $QD_1$  then supercurrent shows sinusoidal behaviour and a finite gap is generated between lower and upper ABS at  $\phi = \pm\pi$ . Further increasing the value of interdot hopping, this supercurrent is suppressed. This suppression of supercurrent is because coupling  $QD_1$  with the  $QD_2$ , the electrons tends to tunnel into  $QD_2$ . This causes the interference destruction between two transport channels and as a result the supercurrent decreases. Thus for  $t > 0$ , the system does not acts as a perfect transmitting channel. The suppression of supercurrent can also be explained in terms of the splitting of QDs energy level due to interdot hopping. When  $t \neq 0$ , the equivalent level of QDs splits into two levels i.e.  $\epsilon_{\bar{d}_i} = \epsilon_{d_i} \pm t$ . The equivalent energy level  $\epsilon_{\bar{d}_i}$  moves far away from the Fermi level with increasing interdot hopping and supercurrent decreases.

In figure 4 [(a)-(d)], we plot the total current as a function of superconducting phase difference ( $\phi$ ) for several values of thermal biasing ( $\Delta T$ ) and interdot hopping. First, by decoupling  $QD_2$  form  $QD_1$  (Fig 4 a) the results of S-QD-S system are reproduced [40]. When both  $QD_1$  and  $QD_2$  are coupled, then there is suppression in magnitude of total current with increasing interdot hopping, which is discussed in previous paragraph. In insets 4(b), the individual behaviour of josephson current and quasi-particle current are shown. It is observed that Josephson current is almost independent of thermal biasing ( $\Delta T$ ) and largely depends on superconducting phase difference ( $\phi$ ). On other hand, the quasi-particle current totally depends on the thermal biasing ( $\Delta T$ ). It is important to note that in total current, sinusoidal nature is due to Josephson current and shift in magnitude is due to quasi-particle current. With a increase in interdot hopping, the amplitude of the supercurrent and total current vanishes. In inset 4(d), the behaviour of quasi-particle current is plotted as a function of interdot hopping. It is observed that quasi-particle current first increases with interdot hopping and then attain a maximum value for  $k_B T \sim t$ , and then decreases with further increase in the value of interdot hopping.

In figure 5, we plot the total current as a function of superconducting phase difference ( $\phi$ ) for several values of interdot hopping for finite onsite Coulomb interaction on both dots  $QD_1$  and  $QD_2$ . The Coulomb interaction for both dots is considered the same i.e.  $U_1 = U_2 = U = \Delta_0$ . In the presence of Coulomb interaction, cooper pairs can not tunnel from one superconducting lead to another superconducting lead directly through the quantum dot energy levels because it is unfavourable to occupy the quantum dot with two electrons simultaneously. But electrons or quasi-particle can tunnel one by one through the quantum dot energy levels. This tunneling can generate a supercurrent only when subsequent tunnel events are coherent [14]. This quantum coherent tunneling process can result in a negative or positive supercurrent as shown in figure 5(a). It is observed that, in the presence of finite onsite Coulomb interaction, the magnitude of Josephson supercurrent as well as total current increases with increasing interdot hopping. We have taken the energy level of quantum dots  $\epsilon_{d_1} = \epsilon_{d_2} = -1.0\Delta_0$ , therefore in the presence of Coulomb interaction, the energy level of quantum dots lies at  $(\epsilon_{d_1}, \epsilon_{d_1} + U)$  and  $(\epsilon_{d_2}, \epsilon_{d_2} + U)$ . Further finite interdot hopping, the equivalent level of QDs splits into two more levels according to  $\epsilon_{\bar{d}_i} = \epsilon_{d_i} \pm t$ . With increasing interdot hopping, the equivalent level of QDs moves close to Fermi level and thus supports the Josephson supercurrent. With increasing interdot hopping, the magnitude of quasi-particle current is small as

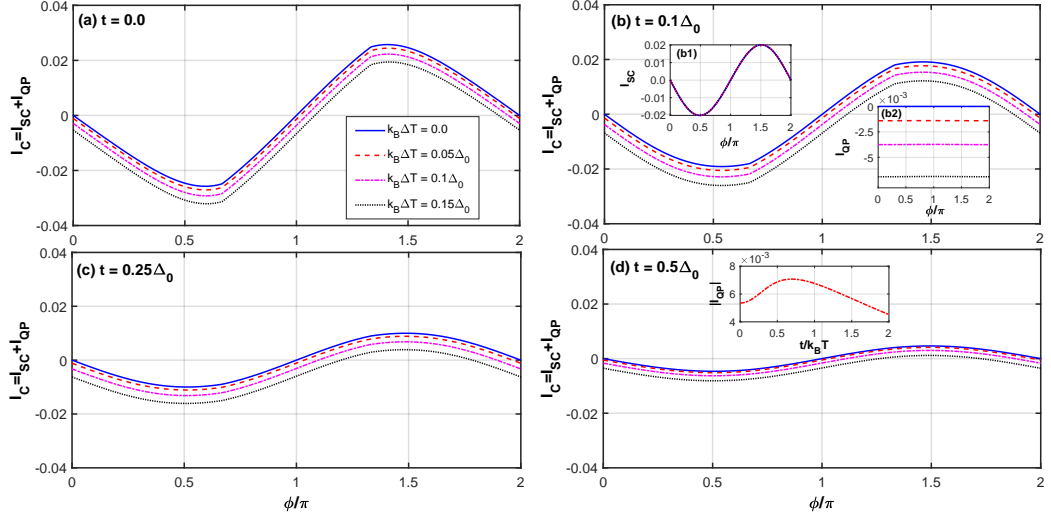


Figure 4: Total current (supercurrent + quasi-particle current) as a function of superconducting phase difference ( $\phi$ ) for different interdot hopping ( $t$ ) and thermal biasing  $\Delta T$ . Insets ( $b_1$ ) and ( $b_2$ ) shows the separate behaviour of Josephson current and quasi-particle current with  $\phi$  and  $\Delta T$ . Inset in figure (d) shows the variation of quasi-particle current as a function of interdot hopping. The other parameters are  $\Gamma = 0.1\Delta_0$ ,  $k_B T = 0.2\Delta_0$ ,  $\epsilon_{d_1} = \epsilon_{d_2} = -1.0\Delta_0$ .

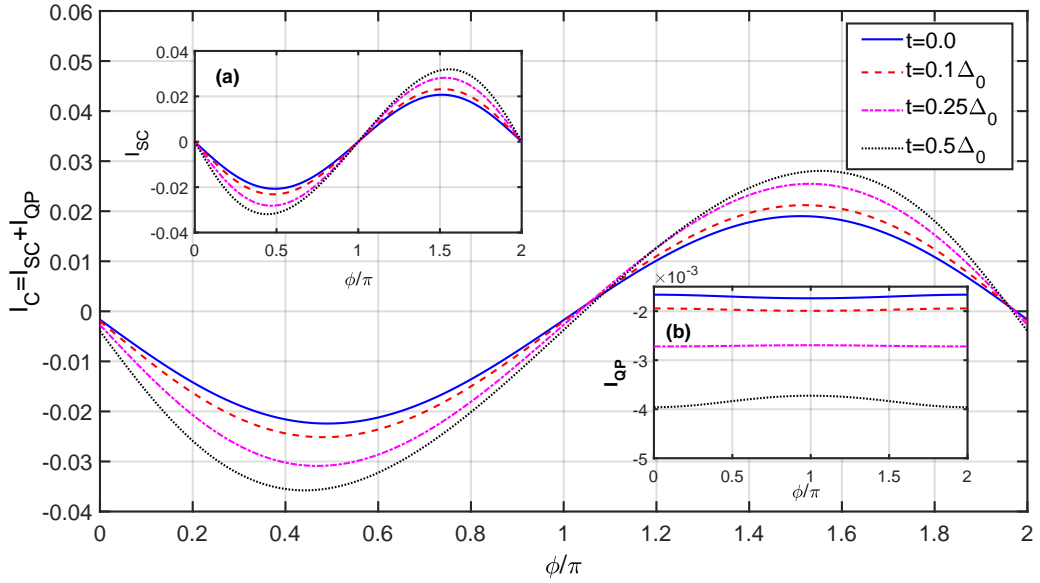


Figure 5: Total current as a function of phase difference ( $\phi$ ) for different interdot hopping ( $t$ ). Insets (a) and (b) shows the separate behaviour of Josephson current and quasi-particle current as a function of  $\phi$  for different  $t$ . Other parameter are  $\Gamma = 0.1\Delta_0$ ,  $k_B T = 0.2\Delta_0$ ,  $\epsilon_{d_1} = \epsilon_{d_2} = -1.0\Delta_0$ ,  $\Delta T = 0.1\Delta_0$ ,  $U = \Delta_0$ .

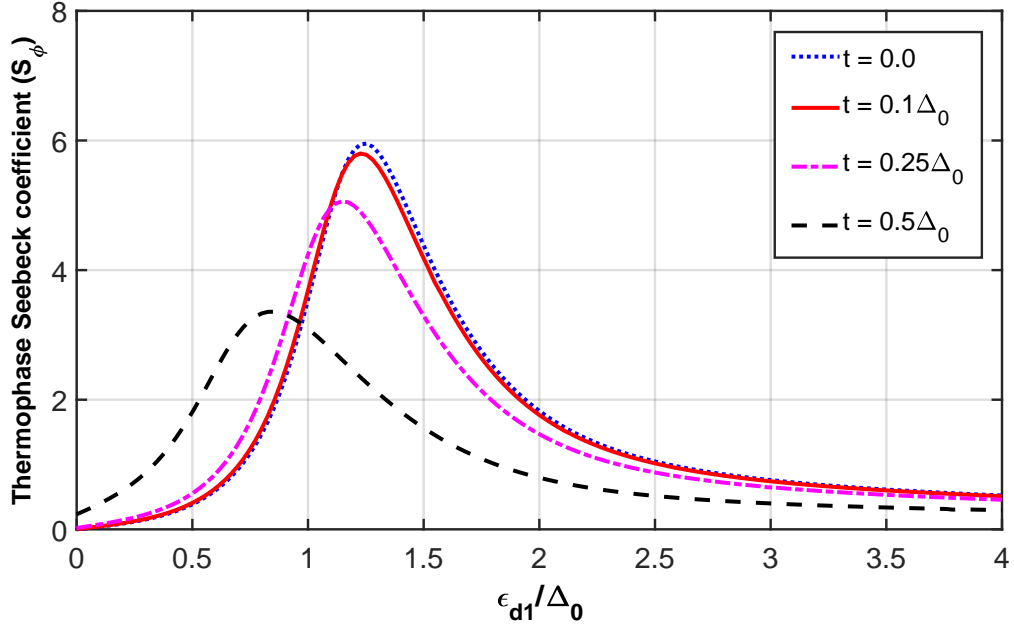


Figure 6: The variation of thermophase Seebeck coefficient ( $S_\phi$ ) with  $QD_1$  energy level  $\epsilon_{d_1}$  for different interdot hopping ( $t$ ). The other parameters are  $U = 0$ ,  $\Gamma = 0.1\Delta_0$ ,  $k_B T = 0.2\Delta_0$ ,  $\epsilon_{d_2} = 0.5\Delta_0$ .

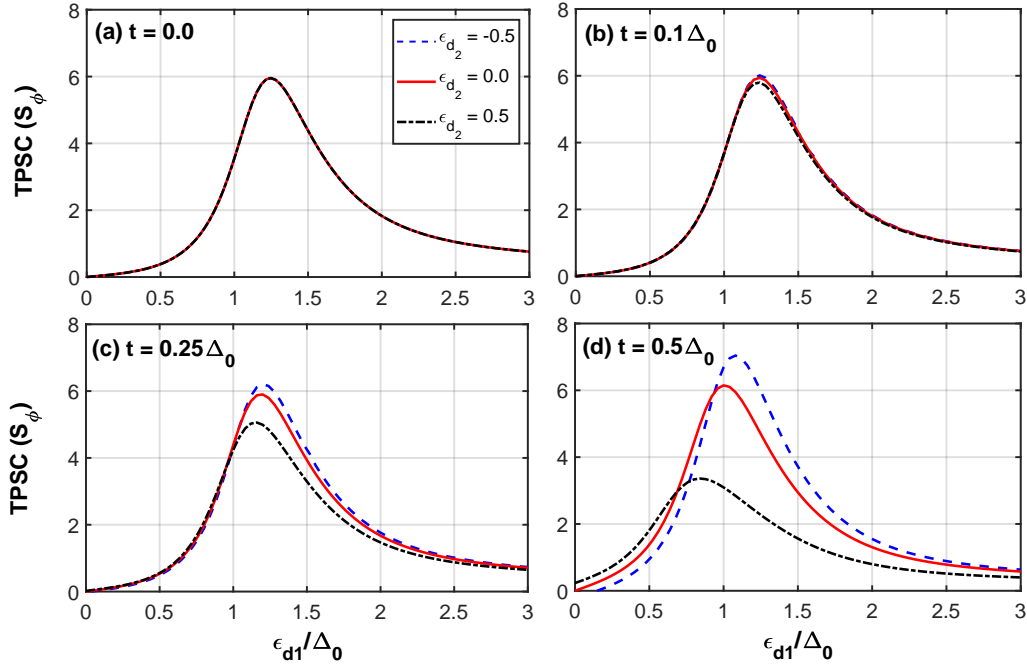


Figure 7: The variation of thermophase Seebeck coefficient ( $S_\phi$ ) with  $QD_1$  energy level  $\epsilon_{d_1}$  for different values of  $QD_2$  energy level  $\epsilon_{d_2}$  and  $t$ . The other parameters are  $U = 0$ ,  $\Gamma = 0.1\Delta_0$ ,  $k_B T = 0.2\Delta_0$ .

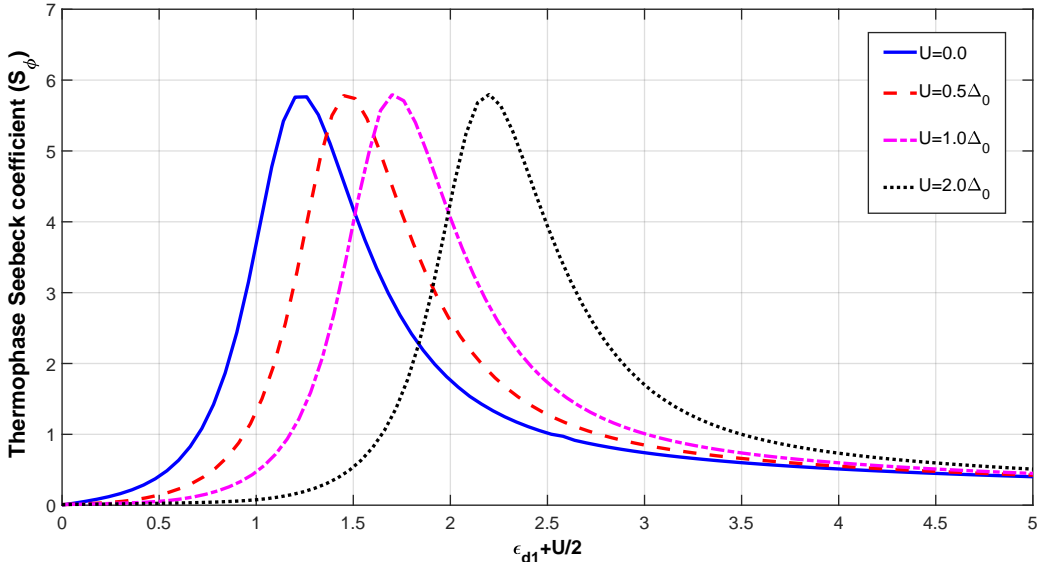


Figure 8: Thermophase Seebeck coefficient as a function of  $QD_1$  energy level for different values of onsite Coulomb interaction. Other parameters are  $t = 0.1\Delta_0$ ,  $k_B T = 0.2\Delta_0$ ,  $\Gamma = 0.1\Delta_0$ ,  $\epsilon_{d_2} = 0.5\Delta_0$

compared to Josephson supercurrent and it produces a small shift from  $\phi = \pi$  in total current.

As discussed previously, the origin of thermophase effect is due to the vanishing total current in open circuit configuration i.e. thermal driven quasi-particle current is compensated by the phase driven Josephson supercurrent flowing in the reverse direction. In figure 6, 7 and 8, we have analyzed thermophase seebeck coefficient ( $S_\phi$ ) of S-TDQD-S in linear response regime for uncorrelated and correlated quantum dots.

In figure 6, we have plot the thermophase Seebeck coefficient (TPSC) as a function of  $QD_1$  energy level for different interdot hopping. It is observed that TPSC ( $S_\phi$ ) peaks are highest for  $t=0$  i.e., when  $QD_2$  is decoupled from  $QD_1$  [40]. When  $QD_2$  is coupled with  $QD_1$ , TPSC peaks starts decreasing with increasing interdot hopping ( $t$ ). To achieve high thermophase peak Josephson current should compensate the quasi-particle current totally. As we have shown that Josephson supercurrent decreases with increasing interdot hopping in the absence of coulomb interaction, therefore it compensates less quasi-particle current. Thus, TPSC peaks decreases and produce a shift in peaks with increasing interdot hopping.

The magnitude of TPSC not only depends on interdot hopping but also depends on the position of  $QD_2$  energy levels whether it lies above or below the Fermi level. In figure 7, we plot the thermophase Seebeck coefficient ( $S_\phi$ ) as a function of  $QD_1$  energy level for different values of  $QD_2$  energy level. When  $QD_2$  is decoupled from  $QD_1$ , then system reproduces the results of S-QD-S for TPSC ( $S_\phi$ ). For finite interdot hopping, the magnitude of TPSC peaks are enhanced when  $QD_2$  energy level lies below the Fermi level. The enhancement of TPSC peaks can be explained as follows: when  $QD_2$  energy level lies below the Fermi level, the equivalent or effective level lies close to the Fermi level which supports the resonant cooper pair tunneling. Therefore thermally induced quasi-particle is compensated by Josephson supercurrent completely i.e. large magnitude of TPSC peaks. These results for different values of  $QD_2$  energy levels can be directly compared with the TPSC plots as discussed in figure (6). In figure 8, We plot the effect of Coulomb interaction in TPSC. In the presence of finite Coulomb interaction on both quantum dots the magnitude of TPSC peaks are unaffected and only a trivial shift of  $\frac{U}{2}$  from  $U = 0$  peak is observed.

## 4 Conclusion

We have addressed the phase-driven and thermal-driven transport properties through a T-shaped double quantum dot Josephson junction. Initially, for uncorrelated quantum dots, the impact of interdot hopping on Andreev bound states (ABS) and Josephson supercurrent are investigated. For a finite value of interdot hopping, Josephson supercurrent exhibits sinusoidal nature while ABS shows a finite gap around the Fermi level. The magnitude of Josephson supercurrent decreases with increasing interdot hopping because the electrons have a tendency to tunnel into side dot with increasing interdot hopping, which results in interference destruction between two transport channels. Further, this system exhibits a finite thermal response when a small thermal biasing ( $\Delta T$ )

is applied across the superconducting leads. The quasi-particle current flows across the junction due to thermal biasing, while the Josephson current is almost insensitive to thermal biasing. With increasing thermal biasing, the quasi-particle current produces a finite shift in the magnitude of the total current. Also, in the absence of onsite Coulomb interaction, the magnitude of the total current decreases with increasing interdot hopping because the equivalent level of quantum dots moves further away from the Fermi level and thus cooper pair tunneling is suppressed. However, when onsite Coulomb interaction is present, electrons or quasi-particles tunnel through the quantum dot energy levels one by one. This tunneling can generate a supercurrent only when subsequent tunnel events are coherent. A positive or negative supercurrent is produced in the system as a result of this quantum coherent tunnelling. Also, for finite Coulomb interaction, the equivalent quantum dot energy levels move towards the Fermi level with increasing interdot hopping, and the magnitude of the Josephson supercurrent or total current increases.

Finally, we investigate the influence of interdot hopping, onsite Coulomb interaction, and quantum dot energy levels on the thermophase Seebeck coefficient (TPSC). In the absence of onsite Coulomb interaction, the magnitude of TPSC ( $S_\phi$ ) decreases with increasing interdot hopping when the energy levels of the side dot ( $QD_2$ ) lie above the Fermi level and increases when energy levels of side dot ( $QD_2$ ) lie below the Fermi level. In the later case, when energy levels lie below the Fermi level, the equivalent level ( $\epsilon_{d_i} \pm t$ ) of quantum dot moves towards the Fermi level. Thus, the cooper pair tunneling increases with interdot hopping, and quasi-particle current is completely compensated by the Josephson current and the magnitude of TPSC peaks is enhanced. It is also observed that the magnitude of TPSC peaks is unaffected by the presence of onsite Coulomb interaction but only a shift of  $\frac{U}{2}$  occurs in TPSC peaks.

We believe that the results presented in this study can be tested experimentally with the advancement in nano-fabrication techniques. The present study can be extended to investigate the thermal transport properties in systems where double quantum dot are coupled with superconducting leads in series and parallel geometry and also for multi-terminal configurations. The concept of thermophase effect in quantum dot-based Josephson junction can be useful for future low-temperature thermal applications [60, 61, 62, 63] and need further investigation.

## Acknowledgments

The authors acknowledge the financial support from the research project DST-SER-1644-PHY 2021-22. Bhupendra Kumar also acknowledge the support from the Ministry of Education (MoE), India, in the form of PhD fellowship.

## References

- [1] B. D. Josephson, Possible new effects in superconductive tunnelling, *Physics Letters* 1 (1962) 251–253. doi:10.1016/0031-9163(62)91369-0.
- [2] P. W. Anderson, How josephson discovered his effect, *Phys. Today* 23 (11) (1970) 23–29. doi:10.1063/1.3021826.
- [3] L. P. Kouwenhoven, D. Austing, S. Tarucha, Few-electron quantum dots, *Reports on Progress in Physics* 64 (6) (2001) 701. doi:10.1088/0034-4885/64/6/201.
- [4] M. A. Kastner, Artificial atoms, *Physics Today* 46 (1993). doi:10.1063/1.881393.
- [5] A. Rozhkov, D. P. Arovas, Josephson coupling through a magnetic impurity, *Physical review letters* 82 (13) (1999) 2788. doi:10.1103/PhysRevLett.82.2788.
- [6] E. Vecino, A. Martín-Rodero, A. L. Yeyati, Josephson current through a correlated quantum level: Andreev states and  $\pi$  junction behavior, *Physical Review B* 68 (3) (2003) 035105. doi:10.1103/PhysRevB.68.035105.
- [7] M.-S. Choi, M. Lee, K. Kang, W. Belzig, Kondo effect and josephson current through a quantum dot between two superconductors, *Physical Review B* 70 (2) (2004) 020502. doi:10.1103/PhysRevB.70.020502.
- [8] J. S. Lim, M.-S. Choi, Andreev bound states in the kondo quantum dots coupled to superconducting leads, *Journal of Physics: Condensed Matter* 20 (41) (2008) 415225. doi:10.1088/0953-8984/20/41/415225.
- [9] Y. Zhu, Q.-f. Sun, T.-h. Lin, Andreev bound states and the  $\pi$ -junction transition in a superconductor/quantum-dot/superconductor system, *Journal of Physics: Condensed Matter* 13 (39) (2001) 8783. doi:10.1088/0953-8984/13/39/307.

- [10] C. Karrasch, A. Oguri, V. Meden, Josephson current through a single anderson impurity coupled to bcs leads, *Physical Review B* 77 (2) (2008) 024517. doi:[10.1103/PhysRevB.77.024517](https://doi.org/10.1103/PhysRevB.77.024517).
- [11] D. Vodolazov, F. Peeters, Superconducting rectifier based on the asymmetric surface barrier effect, *Physical Review B* 72 (17) (2005) 172508. doi:[10.1103/PhysRevB.72.172508](https://doi.org/10.1103/PhysRevB.72.172508).
- [12] Y. Tanuma, Y. Tanaka, K. Kusakabe, Josephson current through a nanoscale quantum dot contacted by conventional superconductors, *Physica E: Low-dimensional Systems and Nanostructures* 40 (2) (2007) 257–260. doi:[10.1016/j.physe.2007.06.008](https://doi.org/10.1016/j.physe.2007.06.008).
- [13] A. Dhyani, B. Tewari, et al., Interplay of the single particle and josephson cooper pair tunneling on supercurrent across the superconducting quantum dot junction, *Physica E: Low-dimensional Systems and Nanostructures* 42 (2) (2009) 162–166. doi:[10.1016/j.physe.2009.09.018](https://doi.org/10.1016/j.physe.2009.09.018).
- [14] J. A. Van Dam, Y. V. Nazarov, E. P. Bakkers, S. De Franceschi, L. P. Kouwenhoven, Supercurrent reversal in quantum dots, *Nature* 442 (7103) (2006) 667–670. doi:[10.1038/nature05018](https://doi.org/10.1038/nature05018).
- [15] K. Grove-Rasmussen, H. I. Jørgensen, P. Lindelof, Kondo resonance enhanced supercurrent in single wall carbon nanotube josephson junctions, *New Journal of Physics* 9 (5) (2007) 124. doi:[10.1021/nl071152w](https://doi.org/10.1021/nl071152w).
- [16] A. Eichler, M. Weiss, S. Oberholzer, C. Schönenberger, A. L. Yeyati, J. Cuevas, A. Martín-Rodero, Even-odd effect in andreev transport through a carbon nanotube quantum dot, *Physical review letters* 99 (12) (2007) 126602. doi:[10.1103/PhysRevLett.99.126602](https://doi.org/10.1103/PhysRevLett.99.126602).
- [17] Y. Ma, T. Cai, X. Han, Y. Hu, H. Zhang, H. Wang, L. Sun, Y. Song, L. Duan, Andreev bound states in a few-electron quantum dot coupled to superconductors, *Physical Review B* 99 (3) (2019) 035413. doi:[10.1103/PhysRevB.99.035413](https://doi.org/10.1103/PhysRevB.99.035413).
- [18] J.-D. Pillet, P. Joyez, M. Goffman, et al., Tunneling spectroscopy of a single quantum dot coupled to a superconductor: From kondo ridge to andreev bound states, *Physical Review B* 88 (4) (2013) 045101. doi:[10.1103/PhysRevB.88.045101](https://doi.org/10.1103/PhysRevB.88.045101).
- [19] E. J. Lee, X. Jiang, M. Houzet, R. Aguado, C. M. Lieber, S. De Franceschi, Spin-resolved andreev levels and parity crossings in hybrid superconductor–semiconductor nanostructures, *Nature nanotechnology* 9 (1) (2014) 79–84. doi:[10.1038/nnano.2013.267](https://doi.org/10.1038/nnano.2013.267).
- [20] R. Delagrangé, R. Weil, A. Kasumov, M. Ferrier, H. Bouchiat, R. Deblock,  $0-\pi$  quantum transition in a carbon nanotube josephson junction: Universal phase dependence and orbital degeneracy, *Physical Review B* 93 (19) (2016) 195437. doi:[10.1016/j.physb.2017.09.034](https://doi.org/10.1016/j.physb.2017.09.034).
- [21] D. Szombati, S. Nadj-Perge, D. Car, S. Plissard, E. Bakkers, L. Kouwenhoven, Josephson  $\phi_0$ -junction in nanowire quantum dots, *Nature Physics* 12 (6) (2016) 568–572. doi:[10.1038/nphys3742](https://doi.org/10.1038/nphys3742).
- [22] S.-g. Cheng, Q.-f. Sun, Josephson current transport through t-shaped double quantum dots, *Journal of Physics: Condensed Matter* 20 (50) (2008) 505202. doi:[10.1088/0953-8984/20/50/505202](https://doi.org/10.1088/0953-8984/20/50/505202).
- [23] F. Chi, S.-S. Li, Current–voltage characteristics in strongly correlated double quantum dots, *Journal of applied physics* 97 (12) (2005) 123704. doi:[10.1063/1.1939065](https://doi.org/10.1063/1.1939065).
- [24] Y. Zhu, Q.-f. Sun, T.-h. Lin, Probing spin states of coupled quantum dots by a dc josephson current, *Physical Review B* 66 (8) (2002) 085306. doi:[10.1103/PhysRevB.66.085306](https://doi.org/10.1103/PhysRevB.66.085306).
- [25] R. López, M.-S. Choi, R. Aguado, Josephson current through a kondo molecule, *Physical Review B* 75 (4) (2007) 045132. doi:[10.1103/PhysRevB.75.045132](https://doi.org/10.1103/PhysRevB.75.045132).
- [26] S. Droste, S. Andergassen, J. Splettstoesser, Josephson current through interacting double quantum dots with spin–orbit coupling, *Journal of Physics: Condensed Matter* 24 (41) (2012) 415301. doi:[10.1088/0953-8984/24/41/415301](https://doi.org/10.1088/0953-8984/24/41/415301).
- [27] G. Rajput, R. Kumar, et al., Tunable josephson effect in hybrid parallel coupled double quantum dot–superconductor tunnel junction, *Superlattices and Microstructures* 73 (2014) 193–202. doi:[10.1016/j.spmi.2014.05.029](https://doi.org/10.1016/j.spmi.2014.05.029).

- [28] M. Lee, R. López, R. Aguado, M.-S. Choi, et al., Josephson current in strongly correlated double quantum dots, *Physical review letters* 105 (11) (2010) 116803. doi:10.1103/PhysRevLett.105.116803.
- [29] J. E. Saldaña, A. Vekris, G. Steffensen, R. Žitko, P. Krogstrup, J. Paaske, K. Grove-Rasmussen, J. Nygård, Supercurrent in a double quantum dot, *Physical review letters* 121 (25) (2018) 257701. doi:10.1103/PhysRevLett.121.257701.
- [30] S. De Franceschi, L. Kouwenhoven, C. Schönberger, W. Wernsdorfer, Hybrid superconductor–quantum dot devices, *Nature nanotechnology* 5 (10) (2010) 703–711. doi:10.1038/nnano.2010.173.
- [31] A. Martín-Rodero, A. Levy Yeyati, Josephson and andreev transport through quantum dots, *Advances in Physics* 60 (6) (2011) 899–958. doi:10.1038/nnano.2010.173.
- [32] V. Meden, The anderson–josephson quantum dot—a theory perspective, *Journal of Physics: Condensed Matter* 31 (16) (2019) 163001. doi:10.1088/1361-648X/aafd6a.
- [33] G. D. Guttman, B. Nathanson, E. Ben-Jacob, D. J. Bergman, Thermoelectric and thermophase effects in josephson junctions, *Physical Review B* 55 (18) (1997) 12691. doi:10.1103/PhysRevB.55.12691.
- [34] F. Giazotto, J. Robinson, J. Moodera, F. Bergeret, Proposal for a phase-coherent thermoelectric transistor, *Applied Physics Letters* 105 (6) (2014) 062602. doi:10.1063/1.4893443.
- [35] M. J. Martínez-Pérez, A. Fornieri, F. Giazotto, Rectification of electronic heat current by a hybrid thermal diode, *Nature nanotechnology* 10 (4) (2015) 303–307. doi:10.1038/nnano.2015.11.
- [36] F. Giazotto, T. Heikkilä, F. Bergeret, Very large thermophase in ferromagnetic josephson junctions, *Physical review letters* 114 (6) (2015) 067001. doi:10.1103/PhysRevLett.114.067001.
- [37] G. Marchegiani, P. Virtanen, F. Giazotto, M. Campisi, Self-oscillating josephson quantum heat engine, *Physical Review Applied* 6 (5) (2016) 054014. doi:10.1103/PhysRevApplied.6.054014.
- [38] G. Marchegiani, A. Braggio, F. Giazotto, Phase-tunable thermoelectricity in a josephson junction, *Physical Review Research* 2 (4) (2020) 043091. doi:10.1103/PhysRevResearch.2.043091.
- [39] A. G. Bauer, B. Sothmann, Phase-dependent transport in thermally driven superconducting single-electron transistors, *Physical Review B* 104 (19) (2021) 195418. doi:10.1103/PhysRevB.104.195418.
- [40] Y. Kleeorin, Y. Meir, F. Giazotto, Y. Dubi, Large tunable thermophase in superconductor–quantum dot–superconductor josephson junctions, *Scientific Reports* 6 (1) (2016) 1–7. doi:10.1038/srep35116.
- [41] M. Kamp, B. Sothmann, Phase-dependent heat and charge transport through superconductor–quantum dot hybrids, *Physical Review B* 99 (4) (2019) 045428. doi:10.1103/PhysRevB.99.045428.
- [42] M. Krawiec, Thermoelectric transport through a quantum dot coupled to a normal metal and bcs superconductor, *Acta Physica Polonica A* 114 (2008). doi:10.12693/APhysPolA.114.115.
- [43] S.-Y. Hwang, R. López, D. Sánchez, Cross thermoelectric coupling in normal-superconductor quantum dots, *Physical Review B* 91 (10) (2015) 104518. doi:10.1103/PhysRevB.91.104518.
- [44] S. Verma, A. Singh, Non-equilibrium thermoelectric transport across normal metal–quantum dot–superconductor hybrid system within the coulomb blockade regime, *Journal of Physics: Condensed Matter* 34 (15) (2022) 155601. doi:10.1088/1361-648X/ac4ced.
- [45] S.-Y. Hwang, D. Sánchez, R. López, A hybrid superconducting quantum dot acting as an efficient charge and spin seebeck diode, *New Journal of Physics* 18 (9) (2016) 093024. doi:10.1088/1367-2630/18/9/093024.
- [46] S.-Y. Hwang, R. López, D. Sánchez, Large thermoelectric power and figure of merit in a ferromagnetic–quantum dot–superconducting device, *Physical Review B* 94 (5) (2016) 054506. doi:10.1103/PhysRevB.94.054506.
- [47] S.-Y. Hwang, D. Sánchez, R. López, Nonlinear electric and thermoelectric andreev transport through a hybrid quantum dot coupled to ferromagnetic and superconducting leads, *The European Physical Journal B* 90 (10) (2017) 1–7. doi:10.1140/epjb/e2017-80242-1.

- [48] P. Trocha, J. Barnaś, Spin-dependent thermoelectric phenomena in a quantum dot attached to ferromagnetic and superconducting electrodes, *Physical Review B* 95 (16) (2017) 165439. doi:10.1103/PhysRevB.95.165439.
- [49] W.-P. Xu, Y.-Y. Zhang, Q. Wang, Z.-J. Li, Y.-H. Nie, Thermoelectric effects in triple quantum dots coupled to a normal and a superconducting leads, *Physics Letters A* 380 (7-8) (2016) 958–964. doi:10.1016/j.physleta.2015.12.032.
- [50] H. Yao, C. Zhang, P.-b. Niu, Z.-J. Li, Y.-H. Nie, Enhancement of charge and spin seebeck effect in triple quantum dots coupling to ferromagnetic and superconducting electrodes, *Physics Letters A* 382 (44) (2018) 3220–3229. doi:10.1016/j.physleta.2018.08.033.
- [51] K. I. Wysokiński, Thermoelectric transport in the three terminal quantum dot, *Journal of Physics: Condensed Matter* 24 (33) (2012) 335303. doi:10.1088/0953-8984/24/33/335303.
- [52] G. Michalek, M. Urbaniak, B. Bułka, T. Domański, K. Wysokiński, Local and nonlocal thermopower in three-terminal nanostructures, *Physical Review B* 93 (23) (2016) 235440. doi:10.1103/PhysRevB.93.235440.
- [53] R. Hussein, M. Governale, S. Kohler, W. Belzig, F. Giazotto, A. Braggio, Nonlocal thermoelectricity in a cooper-pair splitter, *Physical Review B* 99 (7) (2019) 075429. doi:10.1103/PhysRevB.99.075429.
- [54] G. D. Guttman, B. Nathanson, E. Ben-Jacob, D. J. Bergman, Phase-dependent thermal transport in josephson junctions, *Physical Review B* 55 (6) (1997) 3849. doi:10.1103/PhysRevB.55.3849.
- [55] H. Haug, A.-P. Jauho, et al., *Quantum kinetics in transport and optics of semiconductors*, Vol. 2, Springer, 2008. doi:10.1007/978-3-540-73564-9.
- [56] L. V. Keldysh, et al., Diagram technique for nonequilibrium processes, *Sov. Phys. JETP* 20 (4) (1965) 1018–1026.
- [57] H. Shiba, A hartree-fock theory of transition-metal impurities in a superconductor, *Progress of Theoretical Physics* 50 (1) (1973) 50–73. doi:10.1143/ptp.50.50.
- [58] D. N. Zubarev, Double-time green functions in statistical physics, *Soviet Physics Uspekhi* 3 (3) (1960) 320. doi:10.1070/pu1960v003n03abeh003275.
- [59] Y. Meir, N. S. Wingreen, Landauer formula for the current through an interacting electron region, *Physical review letters* 68 (16) (1992) 2512. doi:10.1103/PhysRevLett.68.2512.
- [60] F. Giazotto, T. T. Heikkilä, A. Luukanen, A. M. Savin, J. P. Pekola, Opportunities for mesoscopies in thermometry and refrigeration: Physics and applications, *Reviews of Modern Physics* 78 (1) (2006) 217. doi:10.1103/RevModPhys.78.217.
- [61] H. Quan, Y. Wang, Y.-x. Liu, C. Sun, F. Nori, Maxwell’s demon assisted thermodynamic cycle in superconducting quantum circuits, *Physical review letters* 97 (18) (2006) 180402. doi:10.1103/PhysRevLett.97.180402.
- [62] M. Martínez-Pérez, P. Solinas, F. Giazotto, Coherent caloritronics in josephson-based nanocircuits, *Journal of Low Temperature Physics* 175 (5) (2014) 813–837. doi:10.1007/s10909-014-1132-6.
- [63] A. Fornieri, C. Blanc, R. Bosisio, S. D’ambrosio, F. Giazotto, Nanoscale phase engineering of thermal transport with a josephson heat modulator, *Nature nanotechnology* 11 (3) (2016) 258–262. doi:10.1038/nnano.2015.281.